BMT21
3rd International Conference
Business Meets Technology.
Valencia, 23rd & 24th September 2021

EXPERIMENTAL AND NUMERICAL INVESTIGATION OF DISTURBED FLOW PATTERNS BY AN ASYMMETRIC SWIRL GENERATOR

Welsch, Dennis [a1]; Zacharias, Konstantin [a2] and Schlüter, Wolfgang [a3]

[a] *Department of Technology, University of Applied Science Ansbach. Germany.*
([a1] dennis.welsch@hs-ansbach.de, [a2] konstantin.zacharias@hs-ansbach.de,
[a3] wolfgang.schlueter@hs-ansbach.de)

ABSTRACT: In this article a disturbed flow pattern caused by an asymmetric swirl disturbance generator experimentally by laser-Doppler velocimetry (LDV) and numerically by computational fluid dynamics (CFD) is analyzed. From the data collected in experiment and simulation we create, evaluate and compare quantifiable contour and profile plots of the primary flow as well as flow-specific performance indicators in different cross-sections downstream from the disturbance generator. The results show a heavily asymmetric velocity distribution with little to no signs of relaxation over the course of the section of measurements. Significant similarities between measurement and simulation can be observed at small distances downstream from the impediment. Further downstream, with increasing distance, deviations and differences in the flow patterns become more apparent suggesting that the SST turbulence model can only partially reproduce the real flow occurring on the test rig.

KEY WORDS: *CFD; LDV; Asymmetric swirl generator; Flow metering; Performance Indicator.*

1. INTRODUCTION

Pipe systems with elbows, valves, pumps and other devices are found in many industrial applications. All of these elements cause flow disturbances, which lead to different flow patterns besides the fully developed reference profile. Yet, for high accuracy flow measurements, a fully developed flow is mandatory. The knowledge of the disturbance and its relaxation to fully developed flow is important in advising positions for flow meters and estimating volume flow error. The most common elements, such as bends and double-bends out-of-plane, cause rotational velocity fields (swirl) with asymmetric velocity profiles and can have a large impact on flow accuracy (Tawackolian, 2013). Consequently, this flow behavior needs to be emulated in flow meter test benches to approve measurement devices. As a replacement for the current swirl generator in the standards for water meters (OIML R 49) an asymmetric swirl generator as shown in Figure 1 is considered to represent a double bend out-of-plane (Straka *et al.*, 2019).

How to cite: Welsch, D., Zacharias, K., and Schlüter, W. 2021. Experimental and numerical investigation of disturbed flow patterns by an asymmetric swirl generator. In Proc.: *3rd International Conference Business Meets Technology*. Valencia, 23rd & 24th September 2021. 17-25. https://doi.org/10.4995/BMT2021.2021.13595

The purpose of this study is the comparison of experimental results with corresponding CFD-simulation to validate the SST turbulence model and evaluate the potential for the prediction of experimental results with numerical simulations. In this context, performance indicators are calculated to compare the numerical and experimental results with literature references.

2. MATERIALS AND METHODS

2.1 Experimental set-up

All experiments are performed on a test bench in the flow laboratory of Hochschule Ansbach. For the measurement of the flow patterns downstream from the asymmetric swirl disturbance generator a LDV probe which is mounted on a traversing system for automated displacement is used. The necessary optical access to the section of measurements is realized through a window chamber with a transparent pipe with an inner diameter of D=20.0 mm (and radius R). An 80.0 D straight pipe section upstream from the asymmetric swirl disturbance generator ensures a fully developed flow at its inlet which is confirmed by a preliminary LDV measurement without impediments. LDV data is collected at three different cross-sections with normalized distances z/D=8.5, z/D=12.0 and z/D=19.0 downstream from the asymmetric swirl disturbance generator.

At each cross-section the axial velocity component $\overline{w}$ in z-direction and the tangential velocity components $\overline{u}$ and $\overline{v}$ in x- and y-direction are measured respectively in each of the 281 points of the measurement grid shown on the left-hand side of Figure 1. For each grid point the mean velocity components $\overline{u}$, $\overline{v}$ and $\overline{w}$ re computed from a large number of individual samples measured (up to n_{max}=3·10^3) during the measurement time t_{max}=30 s . The set-up for measuring the axial velocity is illustrated on the right-hand side of Figure 1 along with the directions of the chosen coordinate system and the perspective of observation.

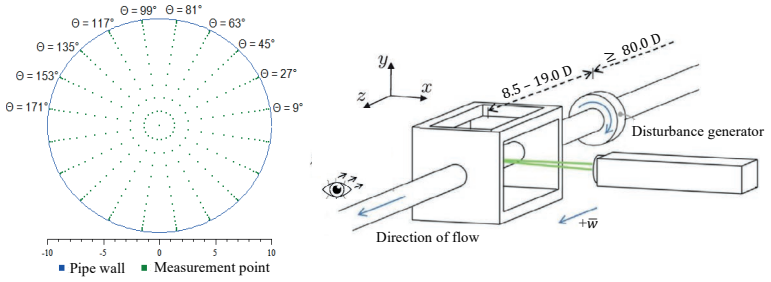

Figure 1. LDV measurement grid with ten profile paths from 9° to 171° (left). Experimental set-up for measuring the axial velocity component (right, own illustration based on Turiso et al., 2018).

2.2 Numerical set-up

The corresponding numerical simulation is performed using the CFD software Simcenter Star-CCM+. In the steady simulation the Reynolds-averaged Navier-Stokes equations are solved by the Segregated Flow Solver using the SST (Menter) k-ω turbulence model. The computational domain has a total length of 570 mm and is depicted in Figure 2. The asymmetric swirl disturbance generator is placed at 6.25 D downstream from the inlet. The volume mesh is realized with a total of 3,508,742 unstructured polyhedral cells including a prism-layer for the near-wall region and a global non dimensional wall distance $y^+<1$. Consequently, the boundary layer is directly resolved in a low-y^+ approach without a wall function. A fully developed turbulent flow matching the experimental boundary conditions is modelled and used as an inlet condition.

In simulation and experiment we consider the same three cross-sections downstream from the modelled disturbance generator for a reasonable comparison (Figure 2).

2.3 Flow conditions

The simulation and all measurement series are conducted with a constant volumetric flow rate of $\dot{Q}$=2.25 m^3/h and a constant water temperature of T=25.0°C. The kinematic viscosity is $\upsilon(25°C)=0.893\cdot10^{-6}$ m^2/s . This results in a volumetric velocity of w_{vol}=1.99 m/s which corresponds to a Reynolds number of $Re=4.5\cdot10^4$.

2.4 Post-processing

Unreliable or erroneous data points from the LDV measurement are identified and evaluated following the method of Hinz (2015) with a criterion of reconstruction of $Tu/\sqrt{n}>\xi$=5.0%, where Tu is the turbulence intensity of any mean velocity component $\overline{\omega}$ and its standard deviation σ_ω and where ξ is the chosen threshold value for admissible standard errors. Measurement points which exceed the threshold are reconstructed by linear interpolation from directly adjacent valid points.

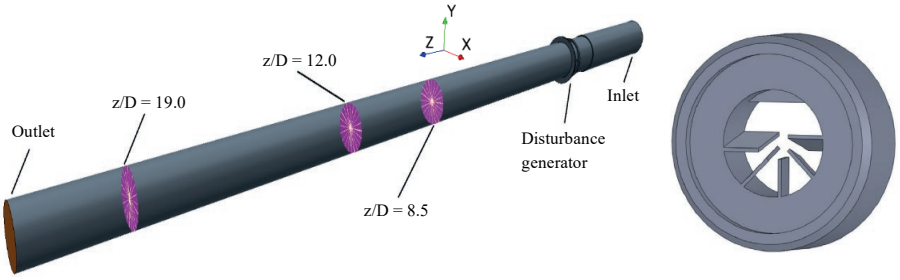

Figure 2: The entire computational domain and the cross-sections considered (left). The asymmetric swirl disturbance generator used (right, Turiso et al., 2018).

Further, the flow-specific metrics K_p, ϕ, K_a and K_{Tu} defined by Yeh and Mattingly (1994) are computed for each cross-sectional plane based on both data sets obtained, LDV measurement and numerical simulation. Each of these performance indicators is obtained as an average value from the profile paths of a cross-section. A more detailed mathematical description can be found in Optolution Messtechnik (2009). For the performance indicators of the LDV data a fully developed turbulent flow profile according to the theory of Gersten and Herwig (1992) is used as a reference profile.

The dimensionless profile factor K_p is a measure of the flatness (K_p<1) or peakness (K_p>1) of the measured or simulated axial flow profile $K_{p,meas}$ compared to a fully developed reference profile $K_{p,ref}$:

$$K_p = \frac{K_{p,meas}}{K_{p,ref}} \tag{1}$$

$$K_{p,meas} = \frac{1}{2 \bullet w_{vol}} \bullet \int_{-1}^{1} \left(\bar{w}_{mid} - \bar{w}\right) d\left(\frac{r}{R}\right) \tag{2}$$

$$K_{p,ref} = \frac{1}{2 \bullet w_{vol,ref}} \bullet \int_{-1}^{1} \left(w_{mid,ref} - w_{ref}\right) d\left(\frac{r}{R}\right) \tag{3}$$

$\overline{w}_{mid}$ and $\overline{w}_{mid,ref}$ are the respective axial velocities at the center of the pipe and $\overline{w}$ and w_{ref} are the respective local axial velocities at the point r/R.

Geometrically, the swirl angle ϕ describes the deviation of a velocity vector from the ideal axial flow direction and thus quantifies the prevailing swirl in a flow. It is computed with the maximum magnitude of the secondary flow $\overline{v}_{xy,max}$ by:

$$\phi = arctan\left(\frac{\bar{v}_{xy,max}}{w_{vol}}\right) \tag{4}$$

The asymmetry factor K_a is a measure of how far the flow profile is offset from the center of the pipe:

$$K_a = \frac{1}{2} \bullet \frac{\int_{-1}^{1} \left(\frac{r}{R} \bullet \bar{w}\right) d\left(\frac{r}{R}\right)}{\int_{-1}^{1} (\bar{w}) d\left(\frac{r}{R}\right)} \tag{5}$$

The dimensionless turbulence factor K_{Tu} is defined as the ratio of the maximum axial turbulence intensity $Tu_{core,max}$ in the core region $-0.2 \leq r/R \leq 0.2$ of the flow and the turbulence intensity $Tu_{mid,ref}$ in the center of the fully developed reference profile:

$$K_{Tu} = \frac{Tu_{core,max}}{Tu_{mid,ref}} \tag{6}$$

3. RESULTS

3.1 Axial flow patterns

The results of the LDV measurement and the simulation are displayed in Figure 3 as normalized contour and profile plots of the axial velocity component $\overline{w}$ at the cross-sections downstream from the asymmetric swirl disturbance generator. The top rows (a), (b), (c) and (g), (h), (i) represent the measured velocity patterns while the bottom rows (d), (e), (f) and (j), (k), (l) belong to the respective numeric solution. Additionally, all profile plots are compared to the fully developed Gersten and Herwig reference profile 'G&H' and the simulated fully developed profile 'Sim FD'.

In the contour plots (a) and (d) at z/D=8.5 we find heavily asymmetric velocity distributions downstream from the disturbance generator which are similar in their basic shape and orientation. The displacement towards the pipe wall in quadrant I and deformation of the kidney-shaped core velocity region is slightly more pronounced in the contour plot of the simulation. Here, the maximum value of the primary flow is reached in profile path 81° in diagram (j) with just 4% difference to the fully developed reference profile. In comparison, the maximum velocity for the measurement at this cross-section is reached in profile path 99° and is 10% lower than the theoretical reference profile according to Gersten and Herwig as illustrated in the corresponding profile plot (g). When comparing the results, it should be noted that the contour plots of the experiment are created by interpolating the discrete data points of the measurement grid. However, the numerical solution uses a much finer computational mesh with more single point values between the defined profile paths. The less defined shape of the core velocity region in contour plot (a) is the consequence of only partially capturing the real flow in the pipe due to low resolution of the chosen grid.

Further downstream, at cross section z/D=12.5, we find a core velocity region in (b) and (e) which has been equally rotated clockwise by approximately 90 degrees. The maximum axial velocity is now reached for both sets of data in the exact same point at x/R = -0.1 und y/R = -0.5 and deviates by 9% for the measurement (previously 10%) and by 6% for the simulation (previously 4%) from the maximum values of the respective reference profiles. For the simulated velocity profile this suggests an increase in flatness with increasing distance from the asymmetric swirl disturbance generator which can also be observed in the more significant differences in the shape of the core flow. In (e) the core flow now occupies a semicircular region in quadrant IV, extending almost over one half of the cross section of the pipe. In the corresponding profile plot (k) the profile paths form an almost even plateau for this region. In comparison, the profile paths of the LDV measurement for this cross-section in (h) are equally flat in the center but fan out less in regions close to the pipe wall. At cross-section z/D=19.0 downstream from the asymmetric swirl disturbance generator the differences between simulation and measurement become more apparent. In contrast to the small core velocity region in (c) the turbulent main flow in (f) is now placed in quadrants I, II and III while receding from the center of the pipe which is also indicated in the profile paths in (l) as a centrally placed local

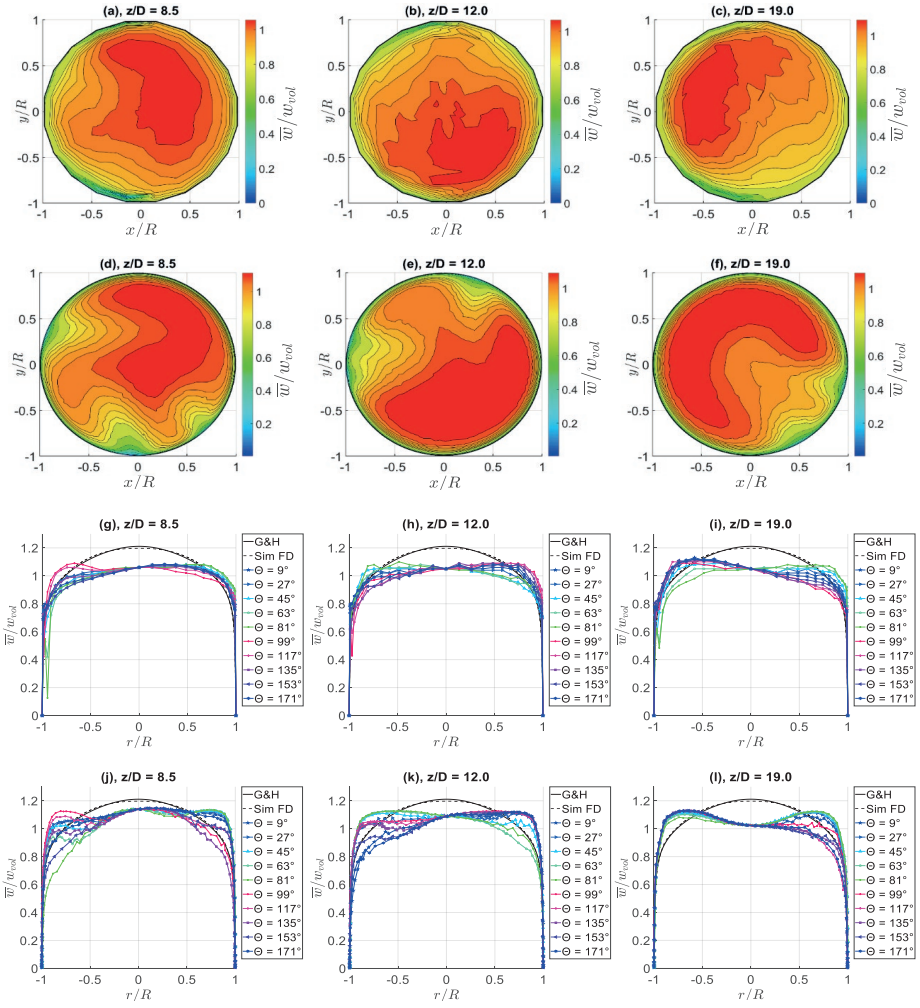

Figure 3: Normalized contour plots of the axial velocity component $\overline{w}$ from the LDV measurement (a), (b), (c) and from the simulation (d), (e), (f). Normalized profile plots of $\overline{w}$ from LDV (g), (h), (i) and from the simulation (j), (k), (l).

minimum. The bundling of the profile paths in the center reflects the approximately radial symmetry of the simulated axial flow profile in quadrants I, II and III. The deviations of the maximum axial velocity from the values of the corresponding reference profile have converged to 5.6% for the measurement and to 6.7% for the simulation. Thus, for the measured velocity distribution a relaxation towards a fully developed profile can be seen (from 10% to 9% to 5.6% deviation). However, both primary flows continue to show a

high degree of turbulence and complexity due to the disturbance of the swirl generator. In a direct comparison of diagrams (c) and (i) with (f) and (l) the significant differences between measurement and simulation are evident. While measurement errors in the LDV are a possible cause for deviating results they often affect only a small number of single measurement points of the grid. The deviations therefore suggest an inadequate modelling of the test rig or simply indicate the limits reached by the selected turbulence model.

3.2 Performance indicators

The following diagrams in Figure 4 depict the flow-specific performance indicators and their respective standard deviation for each cross section downstream from the asymmetric swirl disturbance generator. As a guideline and orientation, the corresponding limit values for a fully developed flow profile are also plotted (gray areas) Optolution Messtechnik (2009). Furthermore, the present results are compared at cross-section z/D=12.0 with selected values from the literature (Turiso et al., 2018) which have been obtained for a similar disturbance generator under slightly varied boundary conditions.

The values for the profile factor in Figure 4 (a) are outside or below the limit value range for an approximately fully developed flow. The highest values, both in the simulation and in the measurement, are reached in the cross-section closest to the disturbance generator downstream at z/D=8.5. The downward trend of the profile factor with increasing distance appears counterintuitive at first but proves consistent with the profile flattening trend observed in Figure 3. It should be noted that low K_p values can also be the result of a displaced core velocity region from the center of the pipe. In the literature we find a profile factor which matches with the present results from the LDV measurement, supporting the plausibility of the calculated values. Overall, the results confirm the interfering influence of the swirl generator on the following flow profile while showing considerable deviations between measurement and simulation.

In contrast, the swirl angle in Figure 4 (b) shows clear parallels between the empirical and numerical sets of data. A similar progressive relaxation of the respective swirl angles can be observed with increasing distance downstream from the disturbance generator, suggesting a decaying behavior of the secondary flow. In the literature a swirl angle ϕ of about 13° is determined which agrees under consideration of the standard deviation at z/D=12.0 with both cases.

The asymmetry factor in Figure 4 (c) shows no predictable trend for either the simulation or the measurement. On average, the axial flow profiles of the simulation have a higher asymmetry factor and are thus more offset from the center of the pipe than the axial velocity profile paths of the measurement which at times even fall into the range of a fully developed flow. A closer inspection of the profile plots, e.g. (k) in Figure 3, reveals individual profile paths that are approximately symmetrical to the center, while other paths intersect the displaced core velocity region only near the wall of the pipe. This results in lower values for the asymmetry factor than one would expect for flows with this level of disturbance and is also the reason for the large standard deviations. The

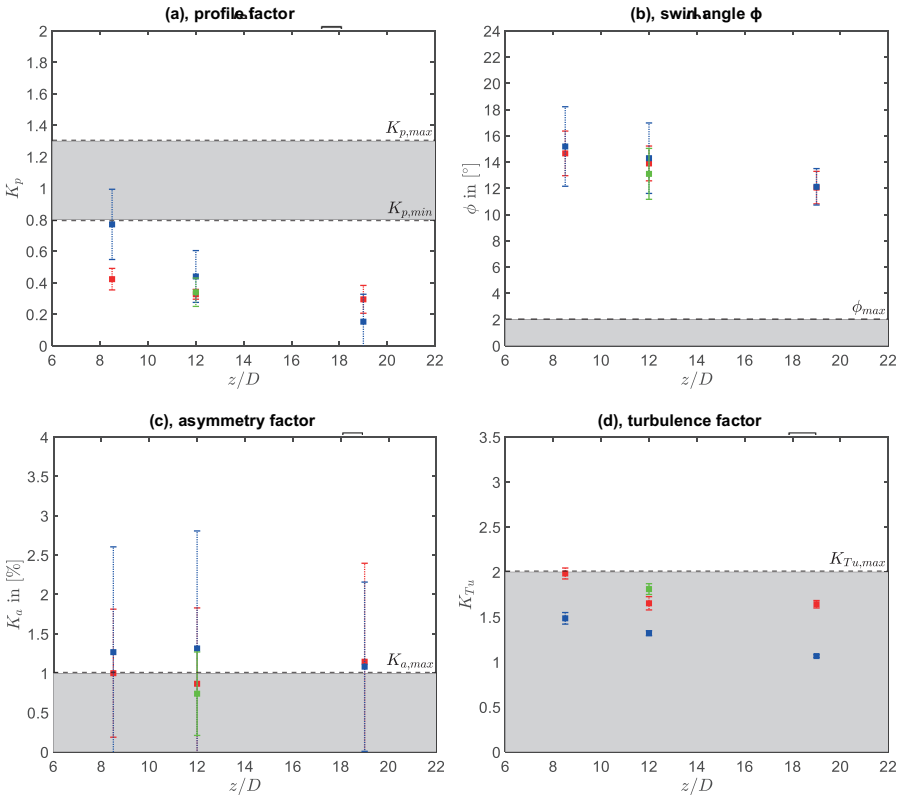

Figure 4. Comparison between LDV measurement ( ), simulation ( ) and previous publica-tion of Turiso et al. [3] ( ) of the performance indicators.

significance of K_a for asymmetrically disturbed flows should therefore be regarded as questionable.

The calculated turbulence factors in Figure 4 (d) fall collectively below the limit for a fully developed flow, with values from the measurement being approx. 30% higher than the values of the simulation across all cross-sections. The characteristic value K_{Tu} can be understood as an estimate of the maximum turbulence intensity occurring in the central region of the pipe. However, in the asymmetric flow field of the disturbance generator the core velocity region is displaced from the center towards the pipe wall. A stronger displacement leads to lower values of K_{Tu} in the considered central region, which is reflected by the deviation between the empirical and numerical values. In the literature we find a value for K_{Tu} which again matches the results from the measurement.

4. CONCLUSION AND OUTLOOK

In this paper, measurements and simulations of a disturbed flow pattern caused by an asymmetric swirl generator were performed. Heavily asymmetric velocity distributions downstream from the swirl generator are found with an increase in flatness in relaxation direction for both cases. In comparison, the profile paths of the LDV measurement are equally flat in the center but fan out less in regions close to the pipe wall. The differences between simulation and measurement become more apparent with increasing distance from the asymmetric swirl disturbance generator. Flow performance indicators obtained from our experiments are in good agreement with the values of Turiso (2018). Comparing measurement and simulation, we see a considerable deviation especially for the profile factor K_p and the turbulence factor K_{Tu}. The results suggest a weakness of the SST turbulence model for asymmetric swirl flows. This is a consequence of the Boussinesq approximation, which assumes isotropic turbulence. However, for further numerical investigations a Reynolds stress equation model (RSM) should be used. This model solves the turbulent transport for all components and should have significantly better accuracy than eddy-viscosity based turbulence models such as the SST turbulence model.

REFERENCES

Gersten, K.; Herwig, G. (1992). Strömungsmechanik. Grundlagen der Impuls-, Wärme- und Stoffübertragung aus asymptotischer Sicht., Vieweg-Verlag, Braunschweig/Wiesbaden.

Hinz, D. F. (2015): Reconstruction of turbulent pipe-flow profiles from laser doppler velocimetry data, *Proceedings of the 15th European Turbulence Conference*, Delft.

Optolution Messtechnik GmbH (2009). Guidelines for the Fluid Mechanical Validation of Calibration Test-Benches in the Framework of EN 1434. Last retrieved May 2021 from https://www.optolution.com/en/service/measurement-services/velocity-profile-analysis-within-the-en-1434/

Straka, M.; Eichler, T.; Koglin, C.; Rose, J. (2019). Similarity of the asymmetric swirl generator and a double bend in the near-field range. *J. Flow Measurement and Instrumentation 70*.

Tawackolian, K. (2013). *Fluiddynamische Auswirkungen auf die Messabweichung von Ultraschall-Durchflussmessgeräten*, Ph.D. thesis, Technische Universität Berlin.

Turiso, M.; Straka, M.; Rose, J.; Bombis, C.; Hinz, D. F. (2018). The asymmetric swirl disturbance generator: Towards a realistic and reproducible standard, *J. Flow Measurement and Instrumentation 60*, S. 144-154.

Yeh, T. T.; Mattingly, G.E. (1994). Pipeflow downstream of a reducer and its effects on flowmeters, *J. Flow Measurement and Instrumentation 5,* S. 181-187.